The Astrophysical Journal Letters, 758:L27 (5pp), 2012 October 20 doi:10.1088/2041-8205/758/2/L27

PERIODIC STRUCTURE IN THE MEGAPARSEC-SCALE JET OF PKS 0637−752

L. E. H. Godfrey[1,2], J. E. J. Lovell[3,4], S. Burke-Spolaor[5], R. Ekers[1,3], G. V. Bicknell[2], M. Birkinshaw[6,7], D. M. Worrall[6,7], D. L. Jauncey[2,3], D. A. Schwartz[6], H. L. Marshall[8], J. Gelbord[9], E. S. Perlman[10], and M. Georganopoulos[11]

[1] International Centre for Radio Astronomy Research, Curtin University, GPO Box U1987, Perth, WA 6102, Australia; L.Godfrey@curtin.edu.au
[2] Research School of Astronomy and Astrophysics, Australian National University, Cotter Road, Weston, ACT 2611, Australia
[3] CSIRO Astronomy and Space Science, Australia Telescope National Facility, P.O. Box 76, Epping, NSW 2121, Australia
[4] School of Mathematics and Physics, University of Tasmania, Private Bag 37, Hobart, Tas 7001, Australia
[5] NASA Jet Propulsion Laboratory, 4800 Oak Grove Drive, Pasadena, CA 91109, USA
[6] Harvard-Smithsonian Center for Astrophysics, 60 Garden Street, Cambridge, MA 02138, USA
[7] HH Wills Physics Laboratory, University of Bristol, Tyndall Avenue, Bristol, BS8 1TL, UK
[8] Kavli Institute for Astrophysics and Space Research, Massachusetts Institute of Technology, Cambridge, MA 02139, USA
[9] Department of Physics, Durham University, South Road, Durham, DH1 3LE, UK
[10] Physics and Space Sciences Department, Florida Institute of Technology, 150 West University Boulevard, Melbourne, FL 32901, USA
[11] Department of Physics, Joint Center for Astrophysics, University of Maryland-Baltimore County, 1000 Hilltop Circle, Baltimore, MD 21250, USA
Received 2012 July 23; accepted 2012 September 17; published 2012 September 27

ABSTRACT

We present 18 GHz Australia Telescope Compact Array imaging of the megaparsec-scale quasar jet PKS 0637−752 with angular resolution ∼0.″58. We draw attention to a spectacular train of quasi-periodic knots along the inner 11″ of the jet, with average separation ∼1.1 arcsec (7.6 kpc projected). We consider two classes of model to explain the periodic knots: those that involve a static pattern through which the jet plasma travels (e.g., stationary shocks) and those that involve modulation of the jet engine. Interpreting the knots as re-confinement shocks implies the jet kinetic power $Q_{\rm jet} \sim 10^{46}$ erg s^{-1}, but the constant knot separation along the jet is not expected in a realistic external density profile. For models involving modulation of the jet engine, we find that the required modulation period is 2×10^3 yr $< \tau < 3 \times 10^5$ yr. The lower end of this range is applicable if the jet remains highly relativistic on kiloparsec scales, as implied by the IC/CMB model of jet X-ray emission. We suggest that the periodic jet structure in PKS 0637−752 may be analogous to the quasi-periodic jet modulation seen in the microquasar GRS 1915+105, believed to result from limit cycle behavior in an unstable accretion disk. If variations in the accretion rate are driven by a binary black hole, the predicted orbital radius is 0.7 pc $\lesssim a \lesssim$ 30 pc, which corresponds to a maximum angular separation of ∼0.1–5 mas.

Key words: galaxies: active – galaxies: jets – quasars: individual (PKS0637−752)

1. INTRODUCTION

The jets of FRII radio galaxies and quasars often exhibit regions of enhanced brightness, commonly referred to as "knots." The production of knots and the associated particle acceleration mechanism are poorly understood (e.g., Stawarz et al. 2004; Niemiec & Ostrowski 2006). Jet knots have traditionally been identified with strong shocks in a uniform and continuous flow. In this class of models, particles are accelerated at the shock via the first-order Fermi mechanism, resulting in a power-law electron energy distribution. Such internal shocks could be formed due to intrinsic velocity irregularities in the jet (Rees 1978), they could be re-confinement/re-collimation shocks (Komissarov & Falle 1998), or they could be associated with large-scale instabilities in the flow (e.g., Bicknell & Begelman 1996). Alternatively, knots in large-scale, powerful radio sources may represent moving and separate portions of the jet matter with higher speed and/or luminosity (Stawarz et al. 2004).

The radio morphology of PKS 0637−752 ($z = 0.653$) consists of a bright core, a knotty, one-sided radio jet extending 15 arcsec west of the core, and a counterlobe 11 arcsec east of the core (see Figure 1). The apparent superluminal motion of parsec-scale jet components with $v/c \approx 13$ implies a jet viewing angle less than 9° (Lovell et al. 2000; Edwards et al. 2006), and hence source size greater than 1 Mpc. The object has received considerable attention in the past decade, largely due to the bright X-ray emission associated with the hundred-kiloparsec-scale western jet. The strong jet X-ray emission is hard to explain in terms of standard emission mechanisms such as thermal Bremsstrahlung or synchrotron self-Compton (Schwartz et al. 2000). As a potential solution to this problem, Tavecchio et al. (2000) and Celotti et al. (2001) proposed the now-popular beamed, equipartition inverse Compton model, in which the cosmic microwave background (CMB) provides the soft photons that are scattered to X-ray energies (IC/CMB model).

Since the launch of *Chandra* in 1999, several tens of quasar X-ray jets similar to PKS 0637−752 have been detected. Despite a decade of intense observational and theoretical analysis, the X-ray emission mechanism, dynamics, and the physical processes shaping jet morphology remain unresolved. A number of problems with the IC/CMB model have been identified (see, e.g., Harris & Krawczynski 2006; Worrall 2009), and while none of the problems is seen as directly refuting the model, mounting criticism has meant that competing models such as dual population synchrotron models (e.g., Tavecchio et al. 2003; Jester et al. 2006) are considered as likely candidates. Additional constraints are required to determine the X-ray emission mechanism and the nature of large-scale quasar jets. In the present work, we consider a new constraint on the jet dynamics: the existence of quasi-periodic peaks in the jet emission. In Section 2, we describe the radio observations and data reduction. In Section 3, we discuss the periodic structure in the jet and possible interpretations.

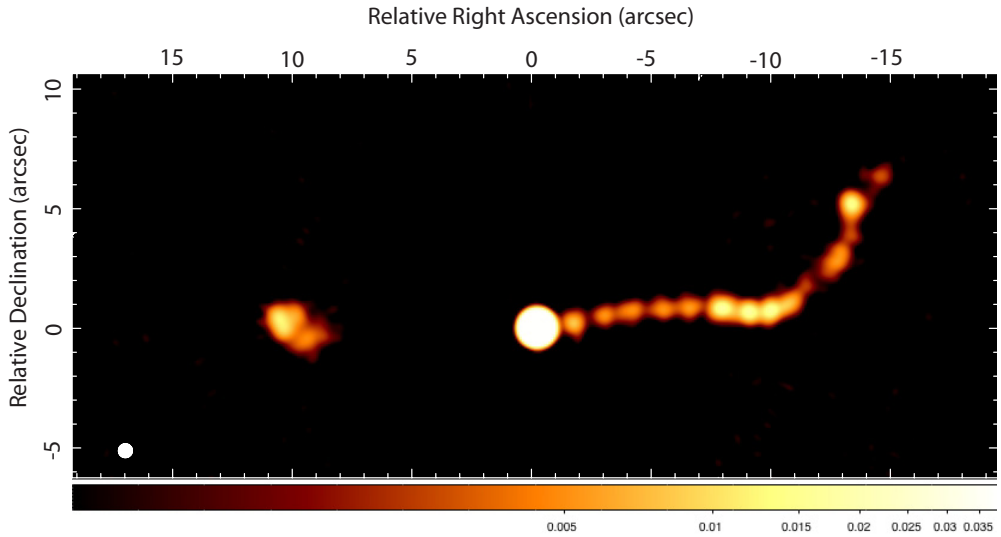

Figure 1. ATCA image of PKS 0637−752 at 17.7 GHz. The color scale is logarithmic between a minimum and maximum surface brightness of 0.5 and 38 mJy beam^{-1}, respectively. This color scale was chosen to show clearly the regular nature of the inner jet knots. The restoring beam is circular with FWHM = 0.″575. The dynamic range is 16,000:1; the off-source rms noise level is 0.3 mJy beam^{-1}, and the peak of the faintest knot in the inner jet is 5 mJy beam^{-1}. Knots in the inner jet are real and are well above the side lobes from the bright core which are at or below the noise level.

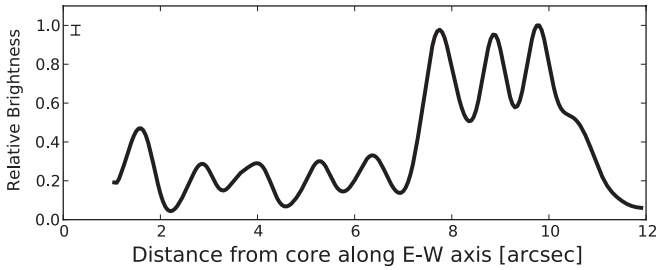

Figure 2. Plot of jet brightness integrated along the north–south direction, as a function of distance from the core in a westerly direction. The bar in the top left of the plot indicates the off-source rms of the projection.

We adopt the following cosmology: $H_0 = 71$ km s^{-1} Mpc^{-1}, $\Omega_m = 0.27$, $\Omega_\Lambda = 0.73$.

2. OBSERVATIONS

PKS 0637−752 was observed with ATCA in the 6C configuration at 17.7 GHz and 20.2 GHz on 2004 May 10. A full 12 hr synthesis was obtained, recording 128 MHz bandwidth. Regular scans on the nearby phase calibrator 0454−810 were scheduled throughout the observations, as well as scans on the ATCA flux calibrator PKS 1934−638. Standard calibration and editing procedures were carried out using the MIRIAD data analysis package. Following the initial calibration, data were exported to DIFMAP and several imaging/self-calibration iterations were performed, incorporating both phase and amplitude self-calibration.

3. PERIODIC JET KNOTS

Trains of bright knots, in some cases with a regular or quasi-periodic pattern, occur in radio galaxy and quasar jets: 3C 175, 3C 204, 3C 263, 3C 334, and 3C303 are prime examples (Bridle et al. 1994; Kronberg 1986). Figures 1 and 2 illustrate the periodic nature of the jet knots in PKS 0637−752, extending along the inner jet up to 11 arcsec from the core. The average apparent knot separation is 1.″1 with standard deviation 0.″15, corresponding to projected separation $D_{\rm app} = 7.6 \pm 1.0$ kpc. Following Mehta et al. (2009), we argue that the jet angle to the line of sight must be greater than ∼4°, otherwise the deprojected source size would be uncomfortably large (>2 Mpc). Based on the Lovell et al. (2000) component identifications and inferred superluminal motion in the parsec-scale jet, Edwards et al. (2006) obtain a limit of $\theta < 9^\circ$ for the jet viewing angle. The parsec-scale and arcsecond-scale radio jets are well aligned (Lovell et al. 2000; Schwartz et al. 2000) so that, unless the jet goes through a large bend in a plane perpendicular to the plane of sky, the jet viewing angle on arcsecond scales is likewise <9°. Thus, if the knots are stationary, the deprojected knot separation is

$$50 \text{ kpc} < D < 110 \text{ kpc}. \quad (1)$$

As discussed in Section 3.2, if the knots are discrete jet components with relativistic velocity then light travel time effects must be taken into account when calculating the knot separation.

The periodic nature of the knots in PKS 0637−752 is striking, and here we ask the question: What physical process is responsible for the periodic knot structure? We can consider the knots to be either (A) a static pattern through which the flow travels (e.g., stationary shocks) or (B) a real variation within the flow caused by a variable jet engine. Section 3.1 deals with models that fall under category A, while Section 3.2 deals with models that fall under category B.

We defer a more detailed investigation to an upcoming publication using spectral index and polarization data based on more sensitive, and higher resolution, ongoing ATCA imaging.

3.1. Large-scale Shocks in a Continuous Flow

3.1.1. Re-confinement Shocks

Hydrostatic jet confinement is accompanied by the formation of regularly spaced shocks along the jet (Sanders 1983; Komissarov & Falle 1998), which could explain the periodic radio structure of PKS 0637−752. Regularly spaced trains of re-confinement shocks are routinely observed in hydrodynamic simulations of active galactic nucleus (AGN) jets (e.g., Aloy et al. 1999; Saxton et al. 2010), and synthetic radio maps based on numerical radiative transfer calculations indicate that simple

luminous knots are associated with the re-confinement, or pinching shocks (Saxton et al. 2010). Analysis of the re-confinement process provides an estimate of the shock separation in terms of the jet power and external pressure. Let ΔR be the separation between re-confinement shocks, $Q_{\rm jet}$ the jet power, and $p_{\rm cocoon}$ the cocoon pressure. Analytic treatment of the re-confinement process, and numerical simulations of axisymmetric, hydrodynamic, relativistic jets indicate that, for a jet with Lorentz factor $\Gamma = 5$,

$$\Delta R \approx 65 \left(\frac{Q_{\rm jet}}{10^{46}\ {\rm erg\ s^{-1}}}\right)^{1/2} \left(\frac{p_{\rm cocoon}}{10^{-11}\ {\rm dyn\ cm^{-2}}}\right)^{-1/2} {\rm kpc}, \quad (2)$$

and is not sensitive to the jet Lorentz factor or jet opening angle (Komissarov & Falle 1998). Croston et al. (2005) find that the typical magnetic field strength in the lobes of high-power FRII radio galaxies is in the order of 10 μG, and that the particle energy density is typically a factor of a few greater than the magnetic energy density. This suggests that the typical lobe pressure is in the order of 10^{-11} dyn cm^{-2}. Therefore, combining Equation (2) with the deprojected knot separation (50 kpc $< D <$ 110 kpc) and an assumed value for the cocoon pressure ($p_{\rm cocoon} \sim 10^{-11}$ dyn cm^{-2}), we find that the re-confinement shock interpretation implies $Q_{\rm jet} \approx 10^{46}$ erg s^{-1}.

Hydrodynamic simulations by Saxton et al. (2010) indicate that the ambient medium influences the distribution of jet knots resulting from re-confinement shocks. In a constant pressure atmosphere, the jet knots remain equally spaced along its length, but in an atmosphere with radially decreasing density, the knots become more closely spaced with distance along the jet. The nearly constant knot separation observed in PKS 0637−752 would therefore require the halo to have a core radius of hundreds of kpc, which is significantly larger than typically observed (Belsole et al. 2007). Furthermore, the re-confinement shock interpretation does not explain why the jet brightens in both the radio and X-ray bands at approximately 8 arcsec from the core. If the difference in jet brightness between the inner and outer jet were due to a difference in jet power, or a difference in cocoon pressure, then we may expect to see this reflected as a difference in knot separation. Instead, we see that the distance between knots remains approximately constant, independent of the jet brightness.

3.1.2. Alternative Mechanisms

A variety of mechanisms have been proposed to explain regular patterns in AGN jets (e.g., Lapenta & Kronberg 2005; Balsara & Norman 1992; Bahcall et al. 1995). Most notably, Kelvin–Helmholtz (KH) instabilities (e.g., Birkinshaw 1990) have been successfully employed to describe the emission patterns in parsec-scale jets (see review by Perucho 2012), as well as the kiloparsec-scale morphology of the jet in M87 (e.g., Bicknell & Begelman 1996; Lobanov et al. 2003). A KH instability interpretation of the regular knot spacings in PKS 0637−752 would imply that the gross structure of the jet changes little over the region where this knot pattern is seen—in particular that the flow speed is constant—consistent with the IC/CMB model for the jet X-ray emission. We defer a more detailed investigation of the KH instability interpretation to an upcoming publication.

3.2. Variation in the Jet Engine

In the following sub-sections, we consider models that invoke modulated activity of the jet engine to explain the semi-regular periodic appearance of the kiloparsec-scale knots. To enable quantitative analysis, we must estimate the modulation timescale. Let us assume that the knots travel with Lorentz factor Γ, at an angle to the line of sight θ. The corresponding Doppler factor is $\delta = [\Gamma(1 - \beta\cos\theta)]^{-1}$. Accounting for projection and light travel time effects, the distance between the jet knots (D) is related to the apparent separation between the knots ($D_{\rm app}$) via

$$D = \frac{D_{\rm app}}{\Gamma\delta\sin\theta}. \quad (3)$$

If the knot velocity $\beta \approx 1$, then $\Gamma\delta\sin\theta \approx \beta_{\rm app}$ where $\beta_{\rm app}$ is the apparent transverse velocity of the kiloparsec-scale knots. Hence,

$$\frac{D_{\rm app}}{\beta_{\rm app,max}} < D < D_{\rm app}\left[\frac{1-\beta\cos\theta}{\sin\theta}\right]_{\rm max}. \quad (4)$$

The apparent transverse velocity of the parsec-scale jet of PKS 0637−752 is $\beta_{\rm app} = 13.3 \pm 1.0$ (Edwards et al. 2006; Lovell et al. 2000). We reasonably assume that the apparent transverse velocity of the kiloparsec-knots is no greater than the apparent transverse velocity of the parsec-scale knots, and therefore argue that $\beta_{\rm app,max} = 13.3$. The one-sidedness of the kiloparsec-scale jet implies that the velocity remains at least mildly relativistic on kiloparsec scales. Based on the current radio and X-ray images, the jet to counterjet brightness ratio is $\gtrsim$60, implying that $\beta > 0.5$. As argued in Section 3, the jet viewing angle is $\theta > 4^\circ$. These limits, combined with Equation (4), imply that if the knots are associated with moving jet components,

$$0.6\ {\rm kpc} < D < 60\ {\rm kpc}, \quad (5)$$

and given $1 < \beta < 0.5$, the inferred modulation period is

$$2 \times 10^3\ {\rm yr} < \tau < 3 \times 10^5\ {\rm yr}. \quad (6)$$

The lower end of this range ($\tau \sim 2 \times 10^3$ yr) is applicable if the jet remains highly relativistic on kiloparsec scales, as suggested by the IC/CMB model of jet X-ray emission (Tavecchio et al. 2000). Given these constraints on the modulation timescale, we now consider two possible physical processes that could result in periodic modulation of the jet engine: accretion disk instabilities and a binary supermassive black hole (SMBH).

3.2.1. Accretion Disk Instabilities

In the context of accretion disk instabilities, we emphasize a possible analogy between the jet of PKS 0637−752 and the quasi-periodic jet modulation in the microquasar GRS 1915+105 in the β state (Fender & Belloni 2004, and references therein). The variations in jet output in GRS 1915+105, with a characteristic timescale of ∼30 minutes, are believed to result from limit cycle behavior in an unstable accretion disk (Janiuk et al. 2002; Janiuk & Czerny 2011; Tagger et al. 2004). Physical timescales are expected to scale linearly with the mass of the black hole, and therefore, the $\tau \sim 30$ minute oscillations in the jet of GRS 1915+105 ($M_{\rm BH} \approx 14\ M_\odot$; Greiner et al. 2001) extrapolate to $\tau \sim 2 \times 10^3$ yr for PKS 0637−752 ($M_{\rm BH} \sim 5 \times 10^8\ M_\odot$; Liu et al. 2006), consistent with the central engine modulation timescale inferred from the periodic structure in the jet.

It has previously been suggested that thermal-viscous instability of the accretion disk may play a role in shaping the morphology of arcsecond-scale AGN jets (e.g., Lin & Shields 1986;

Stawarz et al. 2004). Two modes of thermal-viscous instability potentially operate in accretion disks around massive compact objects: ionization instability and radiation pressure instability (see, e.g., Janiuk & Czerny 2011, for a recent discussion). These instabilities are expected to result in quasi-periodic outbursts due to modulation of the accretion rate, $\dot{M}$. The ionization instability operates in the "partially ionized zone" in the outer disk, where hydrogen transitions from being neutral to ionized. The characteristic ionization instability timescale for SMBHs with $M_{\rm BH} \approx 10^8\ M_\odot$ is $\gtrsim 10^6$ yr (Mineshige & Shields 1990; Janiuk & Czerny 2011), which is longer than the outburst timescale required to explain the periodic structure in the jet of PKS 0637−752.

The radiation pressure instability operates in the inner disk where radiation pressure dominates over gas pressure, and results in shorter timescale variability than the ionization instability (see Janiuk & Czerny 2011). In the context of AGNs, the radiation pressure instability has been proposed as an explanation for the intermittency of radio galaxies on short ($\sim 10^4$ yr) timescales, and in particular, the overabundance of young radio sources in population studies (Reynolds & Begelman 1997; Marecki et al. 2003; Czerny et al. 2009). At high accretion rates (near Eddington), and black hole masses $M_{\rm BH} \sim 10^8$–$10^9\ M_\odot$, the characteristic timescale between outbursts resulting from the radiation pressure instability is $\sim 10^3$–10^4 yr (Merloni & Nayakshin 2006; Czerny et al. 2009)—consistent with the inferred modulation period in PKS 0637−752.

The interplay between the ionization and radiation pressure instability in AGN accretion disks may affect the disk behavior (Siemiginowska et al. 1996; Janiuk & Czerny 2011). Variability over a range of timescales could potentially explain the variation in knot brightness between the inner and outer knots, as well as the variation in brightness between the knot and inter-knot regions.

An alternative instability, the magnetic flooding accretion–ejection instability, has been proposed to explain the β state oscillations in GRS 1915+105, and may be applicable to AGNs (Tagger et al. 2004).

3.2.2. Binary Supermassive Black Hole

In this section, we consider the possibility that the periodic structure in the jet of PKS 0637−752 arises from variations in the accretion rate driven by a binary black hole.

SMBH binaries are expected to result directly from the merger of two massive galaxies, and may populate up to 10% of local galaxies (Volonteri et al. 2003; Burke-Spolaor 2011). However, they are notoriously difficult to detect; no definitive examples have been identified, although several potential binary precursor systems (i.e., dual active nuclei in a single galaxy at large separation) have been confirmed (Komossa et al. 2003; Rodriguez et al. 2006; Fabbiano et al. 2011). Periodicities in morphology, motion, and flux may arise from a bound SMBH pair in a galaxy's center (e.g., Iguchi et al. 2010; MacFadyen & Milosavljević 2008). Excess emission episodes correspond to a secondary SMBH's passage through disk-confined material (gas, stars) around the primary SMBH, inducing a heightened accretion rate at each traversal. Within this interpretation, the oscillatory signal indicates that the secondary SMBH's orbit is not in the same plane as the disk. Given a circular orbit, each observed knot may correspond to one disk passage event. However, if the orbit is elliptical, this model predicts that we are likely to observe double-peaked emission events corresponding to the initial and return traversal through the disk. The spacing of the sub-peaks will depend on the SMBH mass and ellipticity. OJ287, long theorized to be an SMBH binary, shows such structure in its light curve, emitting optical bursts at intervals of 11–12 years, with two sub-peaks per emission cycle (Valtonen et al. 2008). Future high-resolution observations of PKS 0637−752 may reveal additional structure in the jet, such as double peaked knots.

Based on available information, we can estimate the properties of a putative binary system. The knot spacing corresponds either to P (for an elliptical orbit) or $P/2$ (for a circular orbit), where P is the orbital period of the binary system. This leads to periods of $2 \times 10^3 < P < 6 \times 10^5$ years, and assuming a total system mass of $\sim 5 \times 10^8\ M_\odot$ (as estimated by Liu et al. 2006 based on $H\beta$ luminosity and line width), the corresponding orbital radius is 0.7 pc $\lesssim a \lesssim$ 30 pc. This range in orbital radii implies that the largest possible angular separation of the binary lies in the range ∼0.1–5 mas. However, the current projected angular separation of the two SMBHs may be significantly smaller than the maximum angular separation, depending on the orbital orientation and phase.

The binary black hole interpretation cannot explain why the jet brightens in both the radio and X-ray bands at approximately 8 arcsec from the core, and an additional mechanism, such as variation in the jet power, must be invoked to explain the sudden increase in jet brightness at 8 arcsec.

4. DISCUSSION AND CONCLUSIONS

We have presented an 18 GHz ATCA map of the quasar PKS 0637−752, and identified a spectacular train of 9 quasi-periodic knots extending 11 arcsec along the jet. We sought to address the question "What physical process is responsible for the periodic knot structure?," and considered two classes of model: (A) those that involve a static pattern through which the jet plasma travels, and (B) those that involve quasi-periodic modulation of the jet engine. One model that falls under class A is the re-confinement shock interpretation. If the knots are associated with re-confinement shocks, the observed knot separation implies that the jet kinetic power is approximately 10^{46} erg s^{-1}. However, the constant knot separation is not expected in a realistic external density profile. The re-confinement shock interpretation predicts a correlation between knot separation and jet kinetic power, which could be revealed in an imaging survey of a large sample of quasar jets showing regularly spaced knots. In this Letter, we did not consider in detail alternative mechanisms under class A such as KH instabilities. We defer a more detailed investigation of the KH instability interpretation to an upcoming publication.

For models in class B, the quasi-periodic structure in the jet is interpreted as arising from quasi-periodic modulation of the central engine. The inferred modulation period is 2×10^3 yr $< \tau < 3 \times 10^5$ yr. The lower end of this range is applicable if the jet remains highly relativistic on kpc scales, as implied by the IC/CMB model of jet X-ray emission (Tavecchio et al. 2000). This modulation timescale is consistent with the predicted radiation pressure instability timescale in the accretion disks of AGNs. Indeed, we have drawn a direct comparison between the periodic structure in the jet of PKS 0637−752 and the quasi-periodic variation in jet activity seen in the microquasar GRS 1915+105, believed to result from limit cycle behavior in an unstable accretion disk. Finally, variations in the accretion rate may be driven by a secondary black hole in orbit around a primary (i.e., more massive) black hole. We estimated the orbital radius of a putative binary system to be 0.7 pc $\lesssim a \lesssim$ 30 pc,

which corresponds to a potentially resolvable angular separation of ∼0.1–5 mas.

The Australia Telescope Compact Array is part of the Australia Telescope which is funded by the Commonwealth of Australia for operation as a National Facility managed by CSIRO. D.A.S. is supported by NASA contract NAS8-03060 and CXC grant GO9-0121B.

Facility: ATCA

REFERENCES

Aloy, M. A., Ibáñez, J. M., Martí, J. M., Gómez, J.-L., & Muller, E. 1999, ApJ, 523, L125
Bahcall, J. N., Kirhakos, S., Schneider, D. P., et al. 1995, ApJ, 452, L91
Balsara, D. S., & Norman, M. L. 1992, ApJ, 393, 631
Belsole, E., Worrall, D. M., Hardcastle, M. J., & Croston, J. H. 2007, MNRAS, 381, 1109
Bicknell, G. V., & Begelman, M. C. 1996, ApJ, 467, 597
Birkinshaw, M. 1990, in Beams and Jets in Astrophysics, ed. P. A. Hughes (Cambridge: Cambridge Univ. Press), ch. 6
Bridle, A. H., Hough, D. H., Lonsdale, C. J., Burns, J. O., & Laing, R. A. 1994, AJ, 108, 766
Burke-Spolaor, S. 2011, MNRAS, 410, 2113
Celotti, A., Ghisellini, G., & Chiaberge, M. 2001, MNRAS, 321, L1
Croston, J. H., Hardcastle, M. J., Harris, D. E., Belsole, E., Birkinshaw, M., & Worrall, D. M. 2005, ApJ, 626, 733
Czerny, B., Siemiginowska, A., Janiuk, A., Nikiel-Wroczyński, B., & Stawarz, Ł. 2009, ApJ, 698, 840
Edwards, P. G., Piner, B. G., Tingay, S. J., et al. 2006, PASJ, 58, 233
Fabbiano, G., Wang, J., Elvis, M., & Risaliti, G. 2011, Nature, 477, 431
Fender, R., & Belloni, T. 2004, ARA&A, 42, 317
Greiner, J., Cuby, J. G., & McCaughrean, M. J. 2001, Nature, 414, 522
Harris, D. E., & Krawczynski, H. 2006, ARA&A, 44, 463
Iguchi, S., Okuda, T., & Sudou, H. 2010, ApJ, 724, L166
Janiuk, A., & Czerny, B. 2011, MNRAS, 414, 2186
Janiuk, A., Czerny, B., & Siemiginowska, A. 2002, ApJ, 576, 908
Jester, S., Harris, D. E., Marshall, H. L., & Meisenheimer, K. 2006, ApJ, 648, 900
Komissarov, S. S., & Falle, S. A. E. G. 1998, MNRAS, 297, 1087
Komossa, S., Burwitz, V., Hasinger, G., et al. 2003, ApJ, 582, L15
Kronberg, P. P. 1986, Can. J. Phys., 64, 449
Lapenta, G., & Kronberg, P. P. 2005, ApJ, 625, 37
Lin, D. N. C., & Shields, G. A. 1986, ApJ, 305, 28
Liu, Y., Jiang, D. R., & Gu, M. F. 2006, ApJ, 637, 669
Lobanov, A., Hardee, P., & Eilek, J. 2003, New Astron. Rev., 47, 629
Lovell, J. E. J., Tingay, S. J., Piner, B. G., et al. 2000, in Proc. VSOP Symposium, Astrophysical Phenomena Revealed by Space VLBI, ed. H. Hirabayashi, P. G. Edwards, & D. W. Murphy (Sagamihara City: ISAS), 215
MacFadyen, A. I., & Milosavljević, M. 2008, ApJ, 672, 83
Marecki, A., Spencer, R. E., & Kunert, M. 2003, PASA, 20, 46
Mehta, K. T., Georganopoulos, M., Perlman, E. S., Padgett, C. A., & Chartas, G. 2009, ApJ, 690, 1706
Merloni, A., & Nayakshin, S. 2006, MNRAS, 372, 728
Mineshige, S., & Shields, G. A. 1990, ApJ, 351, 47
Niemiec, J., & Ostrowski, M. 2006, ApJ, 641, 984
Perucho, M. 2012, Int. J. Mod. Phys. Conf. Ser., 8, 241
Rees, M. J. 1978, MNRAS, 184, 61P
Reynolds, C. S., & Begelman, M. C. 1997, ApJ, 487, L135
Rodriguez, C., Taylor, G. B., Zavala, R. T., et al. 2006, ApJ, 646, 49
Sanders, R. H. 1983, ApJ, 266, 73
Saxton, C. J., Wu, K., Korunoska, S., et al. 2010, MNRAS, 405, 1816
Schwartz, D. A., Marshall, H. L., Lovell, J. E. J., et al. 2000, ApJ, 540, L69
Siemiginowska, A., Czerny, B., & Kostyunin, V. 1996, ApJ, 458, 491
Stawarz, Ł., Sikora, M., Ostrowski, M., & Begelman, M. C. 2004, ApJ, 608, 95
Tagger, M., Varnière, P., Rodriguez, J., & Pellat, R. 2004, ApJ, 607, 410
Tavecchio, F., Ghisellini, G., & Celotti, A. 2003, A&A, 403, 83
Tavecchio, F., Maraschi, L., Sambruna, R. M., & Urry, C. M. 2000, ApJ, 544, L23
Valtonen, M. J., Lehto, H. J., Nilsson, K., et al. 2008, Nature, 452, 851
Volonteri, M., Haardt, F., & Madau, P. 2003, ApJ, 582, 559
Worrall, D. M. 2009, A&ARv, 17, 1